Numerical Simulation of the Interaction Between Leading-Edge Vortex and Vertical Tail

Donald P. Rizzetta*
U.S. Air Force Wright Laboratory,
Wright–Patterson Air Force Base, Ohio 45433-7913

Introduction

THE impingement of a streamwise vortex on an aerodynamic surface, such as a fin or tail, can result in efficiency loss, severe unsteady loading, vibration, and adverse stability and control. Such vortices, commonly generated by modern fighter aircraft configurations, are employed to supplement lift and enhance performance and maneuvering capabilities in the high-angle-of-attack subsonic flight regime. In these flow situations, vortex breakdown can occur, leading to buffet of the tail surface with a potential for fatigue induced structural failure.

The present investigation considers airflow at a freestream Mach number of 0.2 and root chord Reynolds number of 1.89×10^6 past a sharp leading-edge 70.0-deg swept delta wing at an angle of attack of 23.2 deg. The geometry corresponds to a wind tunnel test model,[1] where twin vertical tails were located on the aft portion of the flat upper surface so as to be impacted by the leading-edge vortices, causing them to break down. Numerical solutions are obtained to the unsteady three-dimensional compressible Euler and mass-averaged Navier–Stokes equations on an overset zonal mesh system. Both the widely used algebraic Baldwin–Lomax[2] closure model, and a two-equation (k–ϵ) representation[3,4] were used to account for effects of turbulence. Although a number of computations have been performed about delta-wing configurations, only recently have two-equation turbulence models been used for such simulations.[5]

Results

A complete description of the calculations, including the governing equations, numerical procedure, generation of meshes, boundary conditions, overset grid treatment, details of the computations, features of the flowfield, and comprehensive results, may be found in Ref. 6. Grid resolution, artificial dissipation, and time-step-size studies also appear therein.

Contours of the streamwise velocity component are shown in Fig. 1. The vertical plane of the contours in Fig. 1a passes through the vertex of the wing along a ray aligned with the chordline of the tail section. Viewing of the contours in the figure is normal to the plane from the inboard side. The vortex core and breakdown region ahead of the tail are clearly visible for the Euler and Baldwin–Lomax solutions, which exhibit an area of reversed streamwise flow indicated by the dark region just upstream of the tail. Because of diffusiveness in the k–ϵ result, the vortex core is poorly defined in this representation and it is obvious that breakdown is absent.

An alternate view of the streamwise velocity component is provided in Fig. 1b. Here the contours have been projected onto a plane that passes through the spanwise coordinate axis at the wing vertex and contains the vortex core trajectory. Contours are viewed in the figure perpendicular to this plane as seen looking down from above. The lateral extent of the breakdown region is apparent. It can also be observed that because the Euler solution lacks the displacement produced by a secondary flow region, the core of the vortex is located farther outboard from that of the Baldwin–Lomax result. Thus, the vortex core in the inviscid case does not impact directly upon the leading edge of the tail. In the Baldwin–Lomax (and k–ϵ) solution, however, the vortex is approximately centered about the tail laterally. This was the flow situation for which the configuration was originally designed.

The diffusiveness in k–ϵ calculation is caused by excessive production of turbulent kinetic energy relative to the dissipation of this energy, particularly within the vortex core region. Because the eddy viscosity is proportional to k^2/ϵ, large values of this coefficient result. It is the large values of eddy viscosity that cause the diffusiveness.

A three-dimensional representation of the wing/tail flowfield is presented in Fig. 2. Crossplane contours and an isosurface of total pressure are displayed from the Baldwin–Lomax solution. Following breakdown, the isosurface appears to wind in a direction opposite to that of the rotational sense of the flow. Areas of reduced total pressure in the lower outboard and midinboard tail regions are

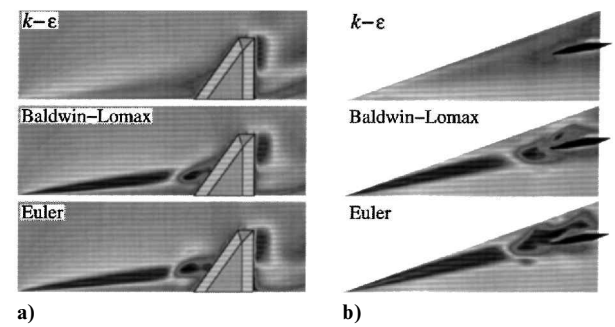

Fig. 1 Contours of streamwise velocity component.

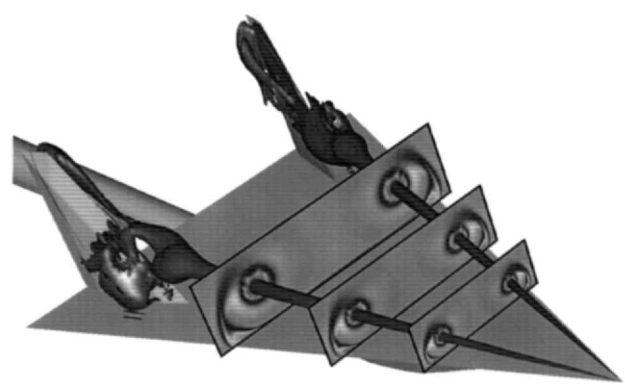

Fig. 2 Crossplane contours and isosurface of total pressure of the Baldwin–Lomax solution.

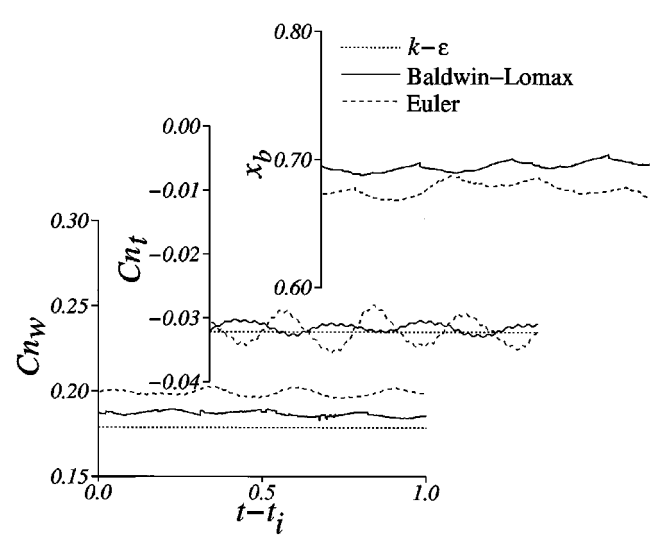

Fig. 3 Time histories of force coefficients and breakdown location.

Received June 14, 1996; presented as Paper 96-2012 at the AIAA 27th Fluid Dynamics Conference, New Orleans, LA, June 17–20, 1996; revision received Dec. 20, 1996; accepted for publication Jan. 13, 1997. This paper is declared a work of the U.S. Government and is not subject to copyright protection in the United States.

*Research Aerospace Engineer, Computational Fluid Dynamics Research Branch, Aeromechanics Division. Associate Fellow AIAA.

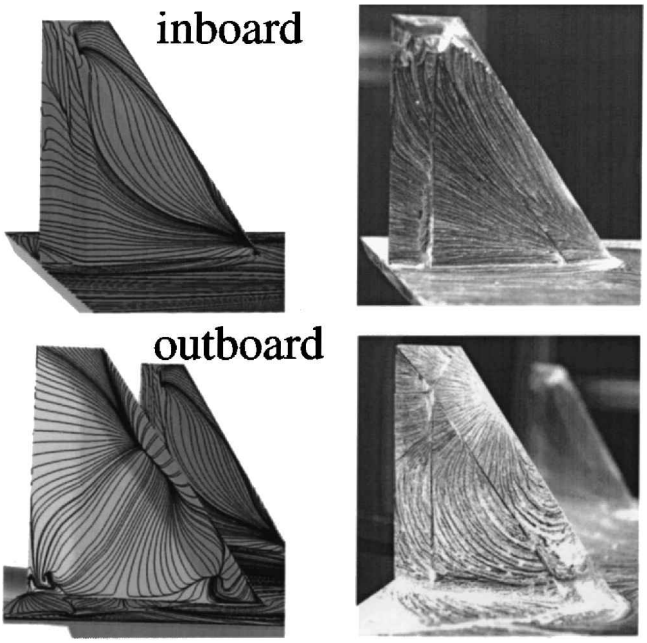

Fig. 4 Comparison of limiting streamline patterns from the Baldwin–Lomax solution with experimental oil flow on the tail surfaces.

apparent in the isosurface. Impact of the vortex on the tail precludes any further winding of the isosurface downstream.

Time histories of the integrated normal force coefficients on the wing (Cn_w) and tail (Cn_t) surfaces, along with the breakdown location (x_b) are seen in Fig. 3. Breakdown in the Euler solution occurs upstream from that in the Baldwin–Lomax result. In addition, greater amplitudes in the unsteady force coefficients are present for the inviscid computation. Note that although the k–ϵ solution is steady, it produces a force coefficient on the tail surface that is not vastly different from the mean values of the unsteady results. Negative values of Cn_t denote that the force on the tail is directed inboard. Amplitudes of the force coefficients and breakdown location are dominated by a single unsteady mode occurring at a Strouhal number of approximately 2.54, which is associated with the rotational frequency of the vortex core.

Limiting streamlines from the Baldwin–Lomax solution are seen to qualitatively resemble experimental oil flow patterns on the inboard tail surface in Fig. 4. On the outboard surface, the experiment appears to indicate an organized rotational flow, whereas the computation does not. This disparity may be due to deficiencies in the turbulence model for simulating surface flow within a broken down vortex.

Summary and Conclusions

The interaction between a leading-edge vortex and a vertical tail in a high Reynolds number subsonic flow was simulated numerically, considering both the compressible Euler and mass-averaged Navier–Stokes equations. Effects of turbulence were accounted for by employing algebraic and two-equation models. Because of excessive turbulent dissipation, the vortex produced by the k–ϵ equations was larger and weaker than that of the other solutions. As a consequence, no breakdown of the vortex occurred and a steady flowfield resulted. The model, therefore, was incapable of reproducing tail buffet, which is commonly observed.

Both the Euler equations and the Navier–Stokes equations employing the Baldwin–Lomax model resulted in an unsteady interaction. Although the high-frequency unsteady modes, which typify large Reynolds number flowfields, were not present, these equations appear to be useful for practical applications. The vortex size and strength of the two computations was quite similar, but because the Euler solution lacked the displacement produced by the secondary flow region, impact of the vortex was not centered directly upon the tail leading edge as in the experimental design.

Although it is certainly possible to modify the Baldwin–Lomax model for vortical flows about intersecting surfaces using overset grids, this is not a convenient undertaking and requires considerable effort to accomplish. This implementation becomes even less practical as the complexity of the configuration increases. The two-equation model offers an alternative, if the limitations due to excessive dissipation can be overcome. Simple modifications that address this deficiency for delta-wing flowfields are the subject of recent efforts.[5]

Acknowledgments

Computational resources for the work presented here were supported in part by a grant of supercomputer time from the U.S. Department of Defense Major Shared Resource Centers at Vicksburg and Bay St. Louis, Mississippi. The author is indebted to K. J. Moran for assistance with the grid generation, to M. J. Lutton for guidance in running overset grid software, and to T. J. Beutner for supplying details of the experimental investigation. Numerous helpful conversations with R. E. Gordnier, M. R. Visbal, and R. B. Melville are also gratefully acknowledged.

References

[1]Beutner, T. J., Baust, H. N., and Meyers, J. F., "Doppler Global Velocimetry Measurements of a Vortex-Tail Interaction," *Proceedings of the 7th International Symposium on Flow Visualization*, edited by J. P. Crowder, Begell House, New York, 1995, pp. 418–423.

[2]Baldwin, B. S., and Lomax, H., "Thin Layer Approximation and Algebraic Model for Separated Turbulent Flows," AIAA Paper 78-257, Jan. 1978.

[3]Jones, W. P., and Launder, B. E., "The Prediction of Laminarization with a Two-Equation Model of Turbulence," *International Journal of Heat and Mass Transfer*, Vol. 15, No. 2, 1972, pp. 301–314.

[4]Jones, W. P., and Launder, B. E., "The Calculation of Low-Reynolds-Number Phenomena with a Two-Equation Model of Turbulence," *International Journal of Heat and Mass Transfer*, Vol. 16, No. 6, 1973, pp. 1119–1130.

[5]Gordnier, R. E., "Study of a Turbulent Delta-Wing Flowfield using Two-Equation Turbulence Models," AIAA Paper 96-2076, June 1996.

[6]Rizzetta, D. P., "Numerical Simulation of the Interaction Between a Leading-Edge Vortex and a Vertical Tail," AIAA Paper 96-2012, June 1996.

A. Plotkin
Associate Editor